Gene profiling in atherosclerosis reveals a key role for small inducible cytokines: validation using a novel monocyte chemoattractant protein monoclonal antibody

Gene Profiling in Atherosclerosis Reveals a Key Role for Small Inducible Cytokines

Validation Using a Novel Monocyte Chemoattractant Protein Monoclonal Antibody

Esther Lutgens, MD, PhD*; Birgit Faber, PhD*; Kitty Schapira, BSc*; Chris T.A. Evelo, PhD; Rachel van Haaften, PhD; Sylvia Heeneman, PhD; Kitty B.J.M. Cleutjens, PhD; Ann Pascale Bijnens, PhD; Linda Beckers, BSc; J. Gordon Porter, PhD; Charles R. Mackay, PhD; Paul Rennert, PhD; Veronique Bailly, PhD; Matthew Jarpe, PhD; Brian Dolinski, PhD; Victor Koteliansky, MD, PhD; Tony de Fougerolles, PhD; Mat J.A.P. Daemen, MD, PhD

Background—Pathological aspects of atherosclerosis are well described, but gene profiles during atherosclerotic plaque progression are largely unidentified.

Methods and Results—Microarray analysis was performed on mRNA of aortic arches of ApoE$^{-/-}$ mice fed normal chow (NC group) or Western-type diet (WD group) for 3, 4.5, and 6 months. Of 10 176 reporters, 387 were differentially ($>2\times$) expressed in at least 1 group compared with a common reference (ApoE$^{-/-}$, 3- month NC group). The number of differentially expressed genes increased during plaque progression. Time-related expression clustering and functional grouping of differentially expressed genes suggested important functions for genes involved in inflammation (especially the small inducible cytokines monocyte chemoattractant protein [MCP]-1, MCP-5, macrophage inflammatory protein [MIP]-1α, MIP-1β, MIP-2, and fractalkine) and matrix degradation (cathepsin-S, matrix metalloproteinase-2/12). Validation experiments focused on the gene cluster of small inducible cytokines. Real-time polymerase chain reaction revealed a plaque progression–dependent increase in mRNA levels of MCP-1, MCP-5, MIP-1α, and MIP-1β. ELISA for MCP-1 and MCP-5 showed similar results. Immunohistochemistry for MCP-1, MCP-5, and MIP-1α located their expression to plaque macrophages. An inhibiting antibody for MCP-1 and MCP-5 (11K2) was designed and administered to ApoE$^{-/-}$ mice for 12 weeks starting at the age of 5 or 17 weeks. 11K2 treatment reduced plaque area and macrophage and CD45^{+} cell content and increased collagen content, thereby inducing a stable plaque phenotype.

Conclusions—Gene profiling of atherosclerotic plaque progression in ApoE$^{-/-}$ mice revealed upregulation of the gene cluster of small inducible cytokines. Further expression and in vivo validation studies showed that this gene cluster mediates plaque progression and stability. **(*Circulation*. 2005;111:3443-3452.)**

Key Words: atherosclerosis ■ genes ■ inflammation

Although clinical consequences and pathological aspects of atherosclerosis are well described, understanding of the precise molecular mechanisms of atherosclerotic plaque initiation and progression has been a daunting task for years. However, since the 1990s, new techniques have emerged to study gene expression profiles in complex disease systems in high-output fashion.

In atherosclerosis, numerous high-output gene expression studies have been performed in atherosclerosis-related cell types, revealing differential expression of mediators of inflammation, lipid metabolism, signaling molecules, and extracellular matrix–related genes, as well as many unknown genes.[1–5] Although these studies are technically easy to perform, genetic information obtained from cell culture experiments may not accurately reflect the molecular events that take place in an atherosclerotic lesion. A more desirable approach is the use of whole-mount (atherosclerotic) vascular tissue.

Received September 30, 2004; revision received February 7, 2005; accepted March 29, 2005.

From the Departments of Pathology (E.L., B.F., K.S., S.H., K.B.J.M.C., A.P.B., L.B., M.J.A.P.D.) and Bioinformatics (C.T.A.E., R.v.H.), Cardiovascular Research Institute Maastricht, University of Maastricht, Maastricht, the Netherlands; Incyte Corporation, Palo Alto, Calif (J.G.P.); Arthritis and Inflammation Program, Garvan Institute of Medical Research, Darlinghurst, New South Wales, Australia (C.R.M.); and Biogen-Idec Inc, Cambridge, Mass (P.R., V.B., M.J., B.D., V.K., T.d.F.). Drs de Fougerolles and Koteliansky are currently affiliated with Alnylam Pharmaceuticals, Cambridge, Mass.

*The first 3 authors contributed equally to this work.

The online-only Data Supplement can be found with this article at http://circ.ahajournals.org/cgi/content/full/CIRCULATIONAHA.104.510073/DC1.

Correspondence to Esther Lutgens, MD, PhD, Department of Pathology, University of Maastricht, P. Debeyelaan 25, 6229 HX Maastricht, The Netherlands. E-mail e.lutgens@path.unimaas.nl

Circulation **is available at http://www.circulationaha.org** **DOI: 10.1161/CIRCULATIONAHA.104.510073**

In the first whole-mount experiments, gene expression profiles of smooth muscle cell–rich components of the vascular wall (aorta, vena cava, and neointima) were compared on a systematic basis. Comparisons between these different smooth muscle cell origins revealed consistent differential expression of genes encoding matrix proteins (collagens) or proteins involved in G-protein signaling (RGS5).[6,7]

In another set of experiments, gene expression profiles of whole-mount human atherosclerotic plaques[8,9] or macrophages obtained from atherosclerotic plaques by laser microdissection microscopy[10] were compared with nondiseased arterial wall. These studies revealed differential expression of a wide array of genes, the majority of which were involved in foam cell formation, inflammation, apoptosis, and thrombosis.[8–10]

Most acute clinical complications of atherosclerosis result from rupture of an atherosclerotic plaque and superimposed thrombosis.[11,12] Identification of genes correlated with atherosclerotic plaque rupture is crucial to understand and intervene in the disease process. In a recent study we were able to identify genes that were differentially expressed between stable and ruptured human atherosclerotic plaques using the suppression subtractive hybridization technique.[13] Although some clones represented known genes, such as perilipin, the majority of genes found in this study coded for unknown genes, one of which was named *vasculin*.[13,14] In a microarray study that compared coronary atherectomy specimens from patients with stable angina and patients with unstable angina, differential gene expression was predominantly observed in the clusters for thrombosis and inflammation.[15]

The aim of the present study was to obtain a detailed portrait of murine gene expression in the different stages of atherosclerosis. For this purpose we chose microarray (mouse unigene 1, 10 176 reporters, Incyte Corp) analysis. To limit the effects of genetic heterogeneity and environmental influence, the experiment was performed in a well-established mouse model of atherosclerosis, the ApoE$^{-/-}$ mouse. A similar study was performed several years ago, but on a much smaller scale, with limited time points and conditions.[16] In that study, mRNA of entire aortas of ApoE$^{-/-}$ mice fed a Western-type diet for 10 or 20 weeks was hybridized on gene filter arrays containing 588 genes. Multiple gene clusters containing >200 genes based on expression levels were found.[16] In a recent publication, transcripts of aortic tissue of atherosclerosis-resistant (C3H/HeJ) and atherosclerosis-prone (C57Bl6) mice were analyzed at baseline, during aging, and during exposure to an atherogenic stimulus (high-fat diet) and validated in atherosclerotic lesions of ApoE$^{-/-}$ mice, revealing that C57Bl6 mice have an atherosclerosis-prone transcriptional profile.[17]

In our study, gene expression patterns of atherosclerotic aortic arches of ApoE$^{-/-}$ mice that were fed normal chow or a Western-type diet (0.21% cholesterol) for 3, 4.5, and 6 months were determined. Time-related expression pattern clustering and functional grouping of differentially expressed genes revealed an important role of genes involved in inflammation and in protein/matrix degradation. Expression studies further highlighted regulation of the small inducible cytokines during disease development in this murine model. The role of monocyte chemoattractant protein (MCP)-1 and MCP-5 chemokines was validated with the use of a novel monoclonal antibody, which was shown to attenuate atherosclerotic plaque development and progression and to induce plaque stabilization in the ApoE-deficient mouse.

Methods

Microarray

Mice and Experimental Protocols

All animal experiments were performed in accordance with animal care institutional guidelines.

Male ApoE$^{-/-}$ mice were purchased from Iffa Credo (France). Mice were fed either a mouse normal chow diet (NC group) or a Western-type diet (WD group) (0.21% cholesterol, Hope Farms) starting at 5 weeks of age. Mice were killed at the age of 3 months (ApoE$^{-/-}$ NC, n=35; ApoE$^{-/-}$ WD, n=13), 4.5 months (ApoE$^{-/-}$ NC, n=14; ApoE$^{-/-}$ WD, n=14), or 6 months (ApoE$^{-/-}$ NC, n=16; ApoE$^{-/-}$ WD, n=16).

After the experimental period, mice were euthanized after an 8-hour fast, and blood (±1 mL) was drawn from the caval vein for lipoprotein analysis. Mice were used for either RNA or protein extraction (n=10 to 31 per group) or histological analysis (n=4 per group). For RNA or protein extraction, the aortic arches including their main branch points (brachiocephalic artery, left carotid artery, and left subclavian artery) (see Data Supplement Figure) were cleaned from fatty tissue and adventitial tissue, excised, rinsed in ice-cold PBS, snap-frozen in liquid nitrogen, and stored at −70°C until further use. For histological analysis, mice were perfused with PBS containing 1% nitroprusside followed by perfusion with 1% paraformaldehyde as described before.[18] The aortic root and the entire aortic arch including its main branch points were cleaned of fat tissue and fixed overnight in 1% paraformaldehyde.[18] After they were processed, aortic arches were embedded longitudinally, and twenty 4-μm sections that represented the central portion of the aortic arch were cut. For frozen sections (6 μm), aortic roots were embedded in OCT and stored at −70°C.

RNA Isolation and Microarray Analysis

Total RNA was isolated with the use of the RNeasy kit (Qiagen). Per isolation, 3 aortic arches of ApoE$^{-/-}$ mice were pooled. The mean yield per isolation was 5 μg total RNA. For microarray analysis, mRNA was amplified with a T7-based technique.[19]

Microarray Processing

Regulation of gene expression was analyzed with the commercially available cDNA mouse UniGEM array of Incyte Genomics. This array contains 10 176 reporters, representing 9556 genes and 580 controls. Polymerase chain reaction (PCR) analysis confirmed the right identity of 8848 reporters.

Cy3-dUTP or Cy5-dUTP (Amersham) was incorporated during reverse transcription of polyadenylated [poly(A)1] RNA, primed by a dT(16) oligomer, resulting in Cy3- and Cy5-labeled samples.[20] Samples from the experimental groups were labeled with the Cy3 fluorescent dye, and the common reference group was labeled with the Cy5 fluorescent dye.

Microarray Hybridization

cDNA was processed as described before.[20] Briefly, cDNA was applied to the microarray under a coverslip, and the slide was placed in a hybridization chamber that was subsequently incubated for ≈8 to 12 hours in a water bath at 62°C. Subsequently, the slides were washed during 1 minute and dried by centrifugation at 500 rpm.

All samples from the experimental group (3-, 4.5-, and 6-month NC and WD ApoE$^{-/-}$ mice) were hybridized to a cDNA chip and compared with the cohybridized common reference (Figure 1). All hybridizations were performed in duplicate; in total, 2×5 chips were hybridized.

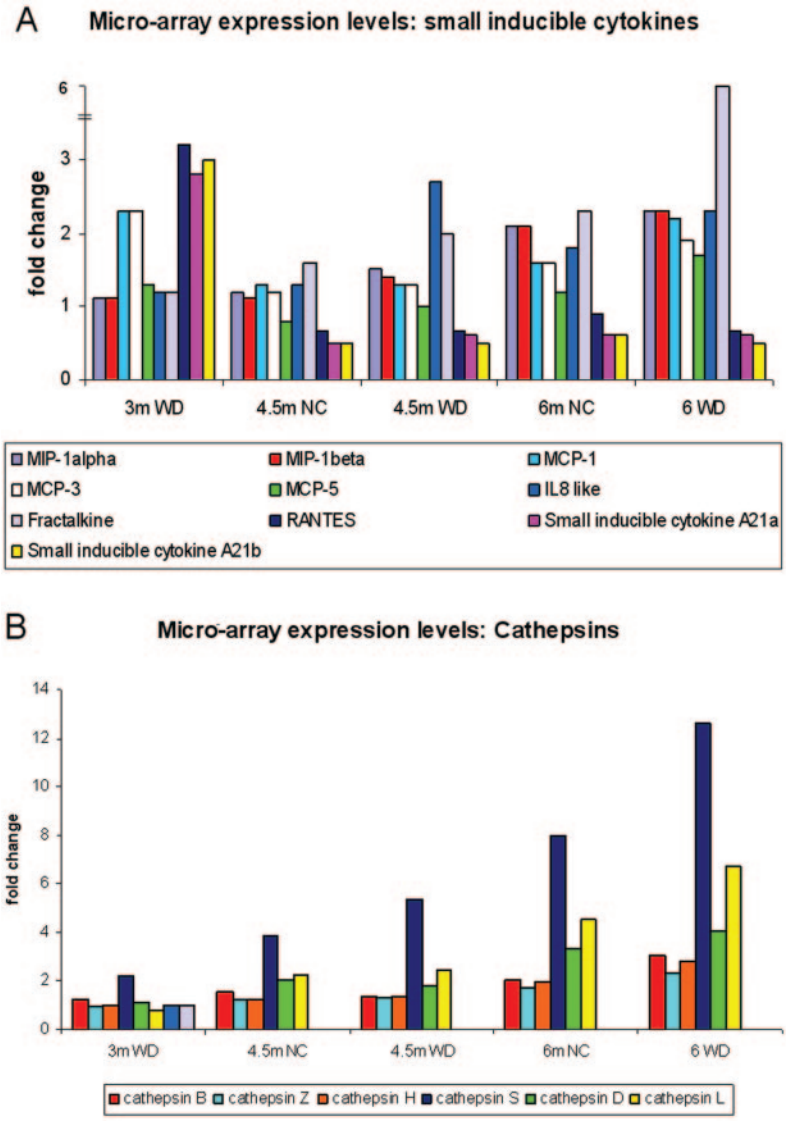

Figure 1. Microarray expression levels of members of the 2 most abundant clusters: small inducible cytokines (A) and cathepsins (B).

(Statistical) Analysis of Microarray Data

Chips were scanned to detect hybridization signals. Scanned image output files were visually examined for major chip defects and hybridization artifacts and subsequently analyzed with Incyte's GemTools software. Genes were analyzed if both of the readings had a signal-to-background ratio of $\geq$2.5, a signal intensity of $>$250 U for 1 or both dyes, and a spot size of $\geq$40% of the spotted area. Twenty-five percent of all arrays contained 1 of 10 176 reporters that failed the minimal area requirement to be included. The mean number of reporters that had a signal below the minimal signal-to-background level was 278.7$\pm$41.6. The threshold of differential expression was set at $>$2-fold upregulation or downregulation.

Subsequently, time-related expression pattern clustering was performed with the use of an algorithm. The different groups representing the different stages of atherosclerosis were put in sequential order on the basis of plaque area, as follows: 3-month WD, 4.5-month NC, 4.5-month WD, 6-month NC, and 6-month WD groups (Data Supplement: Figure and Table I). Subsequently, every gene on each time point was given a number representing $>$2-fold upregulation (1), no change (0), or $>$2-fold downregulation ($-$1) compared with the cohybridized common reference.

Functional grouping of differentially expressed genes was performed with the use of the visualization tool GenMAPP (Gene MicroArray Pathway Profiler; http://www.genmapp.org). This is a generally accessible program for viewing and analyzing microarray data on microarray pathway profiles (MAPPs) representing biological pathways or any other functional grouping of genes.[21] All MAPPs generated from the Gene Ontology database (http://www.geneontology.org) as well as local MAPPS generated by the G-protein Coupled Receptor Database (http://www.gpcr.org), the KEGG database (http://www.genome.ad.jp/kegg), and MAPPs specifically designed for GenMAPP were used. Gene expression data were imported into the program and dynamically linked to the MAPPs with the tool MAPPFinder.

Validation

Quantitative Reverse Transcriptase PCR

The SMART PCR cDNA synthesis kit (BD Sciences) was used for the preparation of double-stranded cDNA from 1 μg template RNA (used from a pool of n=3 aortic arches per group). cDNA was diluted to a total volume of 50 μL. Primers and FAM-TAMRA–labeled probes for mouse MCP-1, MCP-5, macrophage inflammatory protein (MIP)-1α, and MIP-1β were developed. Samples were amplified in duplicate with the use of the Taqman universal PCR master mix and the 7700 sequence detector (Applied Biosystems) with 300 nmol/L of primer and 200 nmol/L of probe. Data were analyzed with the use of Sequence Detection Software (Applied Biosystems). Relative expression of mRNA was calculated by the comparative CT method. To standardize for the amount of input RNA, the endogenous cyclophilin gene was included.

ELISA
Samples of aortic arch were homogenized in tissue protein extract buffer (Pierce) with the use of a Medimachine (BD Biosciences) fitted with 50-μm units. Protein extracts of 2 pools of n=3 aortic arches of ApoE$^{-/-}$ mice per group (3-, 4.5-, and 6-month NC or WD group) were filtered with 30-μm filters and subjected to an ELISA for MCP-1 and MCP-5 (R&D Systems).

Immunohistochemistry
Immunohistochemistry was performed on frozen sections of aortic roots (MCP-1 and MCP-5) or paraffin-embedded aortic arch sections (MIP-1α) with the use of standard procedures. In short, sections were fixed for 15 minutes in 4% paraformaldehyde and incubated with anti–MCP-1 antibody (goat polyclonal, 1:30, R&D Systems), anti–MCP-5 antibody (goat polyclonal, 1:50, R&D Systems), and anti–MIP-1α antibody (rabbit polyclonal, 1:100, RDI) or the respective control IgG (negative control). Subsequently, a suitable biotinylated secondary antibody was applied, followed by incubation with an ABC^{AP} kit (DAKO). Immunostaining was visualized with an alkaline phosphatase-I kit (Vectastain).

Intervention Study

Generation of 11K2 Monoclonal Antibody
Murine hybridomas were generated from RBF mice immunized with human MCP-1 (Garvan Institute) to provide neutralizing monoclonal antibodies. One monoclonal antibody (11K2) was selected for its high affinity for human MCP-1 (14 pmol/L) and its convenient cross-reactivity to the murine homologues (MCP-1 and MCP-5), allowing studies in murine disease models. The 11K2 hybridoma cell line was suspension adapted and grown in reactors, and the antibody was purified by chromatography on protein A Sepharose and SP Sepharose.

ELISA
The wells of a 96-well plate (Maxisorb Nunc) were coated with synthetic murine MCP-1, MCP-3, or MCP-5 (Chemicon). Residual nonspecific binding sites were blocked with BSA. The binding of 11K2 was detected with the use of horseradish peroxidase–conjugated goat anti-murine IgG (Jackson Immunoresearch), and the colorimetric reaction was done with TMB.

Kinexa Assay
The Fab fragment of 11K2 was generated by papain digestion of the antibody and purified from the Fc fragment by chromatography on protein A Sepharose. The affinity of 11K2 for murine MCPs was measured with a Kinexa instrument (Sapidyne Instruments). 11K2 Fab at 20 pmol/L was incubated in PBS, 0.02% azide, 0.1% BSA, with various concentrations of murine MCP-1 (Chemicon Inc) or MCP-5 (Peprotech Inc). The mixtures were allowed to reach equilibrium for 3 hours at room temperature and applied to a column of huMCP-1–coated polymethylmethacrylate beads (98 μm). Free Fab bound to the column and was detected with Cy-5–labeled goat anti-mouse F(ab′)2. Under these conditions, the signal measured is proportional to the concentration of free Fab applied to the column. The data were fit to a quadratic curve fit as described in Hulme and Birdsall.[21a]

Chemotaxis Assays
Chemotaxis toward murine MCP-1 (BioSource), MCP-3, or MCP-5 (Cell Sciences) was measured with the ChemoTx system (Neuro Probe, Inc). Murine monocytes, WEHI-274.1 (ATCC) or THP-1 cells, were separated from the chemokines and the antibody by a filter with 5-μm pores. The effectiveness of 11K2 in inhibiting monocyte chemotaxis was determined after 4 hours. Migration was quantified with Cell Titer dye (Promega).

Mouse Experiments
Male ApoE$^{-/-}$ mice (Iffa Credo) were injected intraperitoneally with the 11K2 antibody (200 μg/wk) or an isotype control antibody (IgG1, MOPC-21) twice a week for 12 weeks. Treatment started at the age of 5 weeks (early treatment: n=15 for 11K2, n=15 for control) or 17 weeks (delayed treatment: n=15 for 11K2, n=15 for control).

Tissue processing was performed as described above, and atherosclerotic lesions were analyzed as described previously.[18,22] In short, atherosclerotic plaques were subdivided into initial lesions (pathological intimal thickening, intimal xanthoma) and advanced lesions (fibrous cap atheroma) according to the classification by Virmani et al.[23] Morphometric analysis, with the use of computerized morphometry (Leica Quantimet 570), included measuring plaque area (hematoxylin-eosin), collagen content (Sirius red), α-smooth muscle actin content (ASMA, mouse monoclonal 1:3000, Sigma), macrophage content (Mac-3, rat monoclonal 1:30, Pharmingen), and CD45^{+} cell content (CD45, rat monoclonal 1:30, Pharmingen).

Evaluation of Possible Side Effects
To evaluate possible side effects of 11K2 treatment, fluorescence-activated cell-sorting (FACS) analysis (FACSCalibur, BD Sciences) with T-lymphocyte–specific antibodies was performed on peripheral blood leukocytes, spleen, and lymph nodes of n=6 11K2- and n=6 control-treated mice of both treatment groups. Antibodies used for staining were CD3^{FITC}, CD4^{Biot}, CD8$^{PE53\text{-}6.7}$, and CD25^{PE} (all from Pharmingen).

In addition, >20 organs were excised and evaluated macroscopically and microscopically on 4-μm sections stained with hematoxylin-eosin.

Lipid Profile
For the assessment of lipid profiles, standard enzymatic techniques were used, automated on the Cobas Fara centrifugal analyzer (Hoffmann–La Roche). Total plasma cholesterol and HDL were measured with the use of kits 07-3663-5 and 543004 (Hoffmann–La Roche); total glycerol with kit 337-40A/337-10B (Sigma); and free glycerol with kit 0148270 (Hoffmann–La Roche). Precipath (standardized serum) was used as an internal standard. LDL was calculated as follows: total cholesterol−[(total glycerol−free glycerol)/2.2)−HDL)].

Statistical Analysis
All microarrays were analyzed and validated with the use of Gemtools. In the intervention study, data were compared with a nonparametric Mann-Whitney *U* test.

Results

Microarray Analysis
In total, 387 of 10 176 reporters were expressed >2-fold (compared with the cohybridized reference: ApoE$^{-/-}$ mice, 3-month NC group) in 1 or more of the experimental groups analyzed. The majority of the differentially expressed genes were upregulated in 1 or more experimental groups (258 genes upregulated, 127 downregulated, 2 upregulated and downregulated in different experimental groups). Of those genes, 289 were known, and 98 were expressed sequence tags (including RIKEN database).

Differential expression levels relative to the cohybridized reference ranged from 2 to 17.5 and from −2 to −11.1. Five genes showed a >10-fold increase, 15 genes >5- to <10-fold, and 240 genes >2- to <5-fold. For the downregulated genes, these numbers were 3, 18, and 109.

Genes that showed the highest relative expression levels were serine protease inhibitor 2-2 (10.5-fold upregulation), CD68 (11.0-fold upregulation), cathepsin S (12.6-fold upregulation), lectin galactose binding soluble 3 (12.4-fold upregulation), and apoptosis inhibitory 6 (17.5-fold upregulation). Genes with the lowest relative expression levels were 3 expressed sequence tags (all −10.1-fold downregulation).

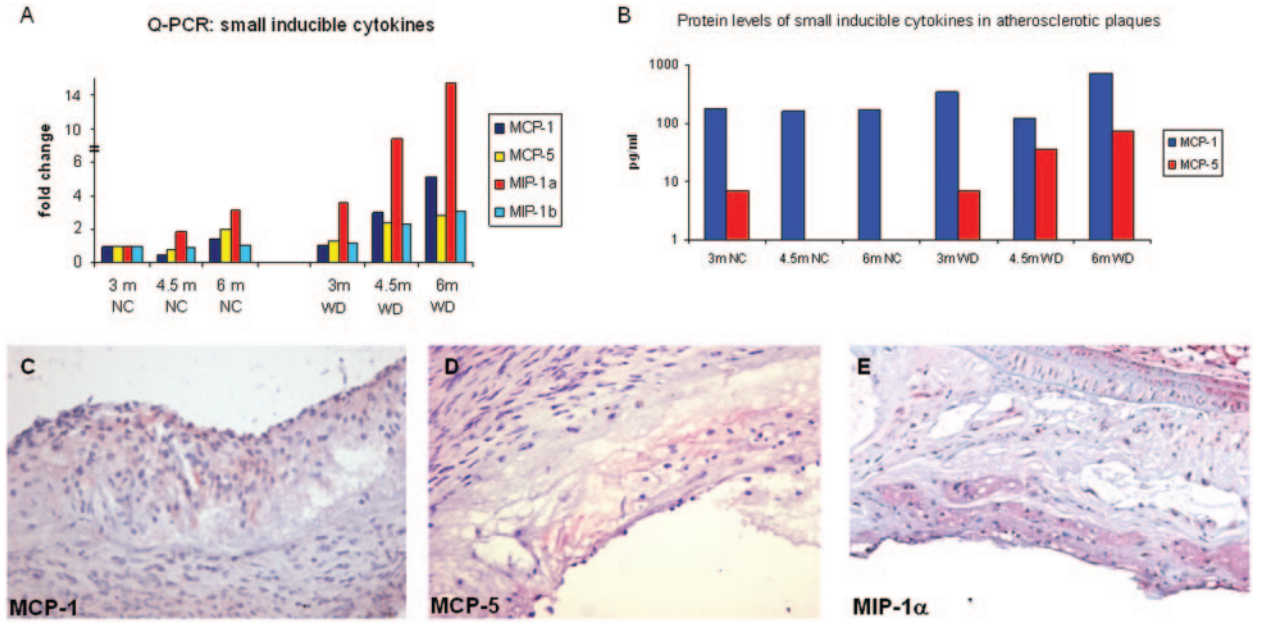

Figure 2. Validation experiments. Quantitative PCR (Q-PCR) (A) and ELISAs (B) show that both RNA and protein levels of several members of the small inducible cytokine family (MCP-1, MCP-5, MIP-1α, and MIP-1β) increase with disease progression. Immunohistochemistry for MCP-1 (C), MCP-5 (D), and MIP-1α (E) (magnification $\times$400) shows that these proteins are predominantly expressed in macrophages of advanced atherosclerotic lesions.

Time-Related Gene Expression Changes During Atherogenesis

For the detection of time-related expression clustering, we developed the algorithm described in Methods. In theory, $3^5=243$ clusters could be formed; however, only 33 different clusters were observed. From these 33 clusters, the majority of genes were found in clusters containing genes upregulated in advanced atherosclerosis. Among those genes, many were linked to inflammation and proteolysis (see Data Supplement Table I).

Functional Grouping of Differentially Expressed Genes

Functional groups that contained most of the differentially expressed genes were those involved in inflammation (acute phase response, chemotaxis, cytokines) and protein/matrix degradation (protein degradation, proteolysis and peptidolysis, catabolism) (see Data Supplement Table II).

Of special interest within these large gene maps were the subfamilies of small inducible cytokines and the cathepsins. Numerous members of both subfamilies were expressed throughout atherogenesis. Members of the small inducible cytokines included MCP-1, MCP-3, MCP-5, RANTES, fractalkine, MIP-1α, MIP-1β, MIP-2, IL-8-like, and small inducible cytokine 21a and 21b. The expression of the majority of the small inducible cytokines was slightly elevated in early atherosclerosis and increased to expression levels above the 2-fold threshold level in advanced atherosclerotic plaques (Figure 1A), except for small inducible cytokine 21a and 21b (CCL21a and b) and RANTES, which appeared to be downregulated in advanced atherosclerosis. Members of the cathepsin subfamily included cathepsin B, D, H, L, S, and Z. Relative expression levels of all members increased steadily during plaque progression (Figure 1B).

Further validation experiments were confined to the small inducible cytokine family.

Validation of Expression Profiles of Small Inducible Cytokines in Atherosclerosis

Real-time PCR for MCP-1, MCP-5, MIP-1α, and MIP-1β on aortic arches of ApoE$^{-/-}$ mice of different age and diet confirmed the increased expression in atherosclerosis (Figure 2A). ELISA on aortic arch lysates showed that expression of MCP-1 and MCP-5 protein was highest in advanced atherosclerotic plaques (Figure 2B). Immunohistochemistry for MCP-1, MCP-5, and MIP-1α showed highest expression levels in macrophage foam cells of advanced atherosclerotic plaques (Figure 2C to 2E).

Role of Small Inducible Cytokines in Atherosclerosis: Mouse Study

11k2: Specificity and Function

The binding specificity of 11K2 was measured by ELISA (Figure 3A). 11K2 demonstrated half-saturable binding at $\approx$1.5 ng/mL (10 nmol/L) for both MCP-1 and MCP-5. In contrast, no specific binding of 11K2 to murine MCP-2 and MCP-3 could be detected up to 10 μg/mL (Figure 3A).

The Fab form of 11K2 was used to obtain a measure of the intrinsic affinity for murine MCP-1 and MCP-5. With the use of Kinexa assay, 11K2 Fab was found to bind to solution phase murine MCP-1 with an affinity of 0.3 nmol/L, whereas its affinity for murine MCP-5 was 1.4 nmol/L (Figure 3B). As observed by ELISA, no binding was observed for murine MCP-2.

The ability of 11K2 to block monocyte chemotaxis was analyzed with the use of cell migration assays. Different ratios of 11K2 and murine MCP-1 or murine MCP-5 were

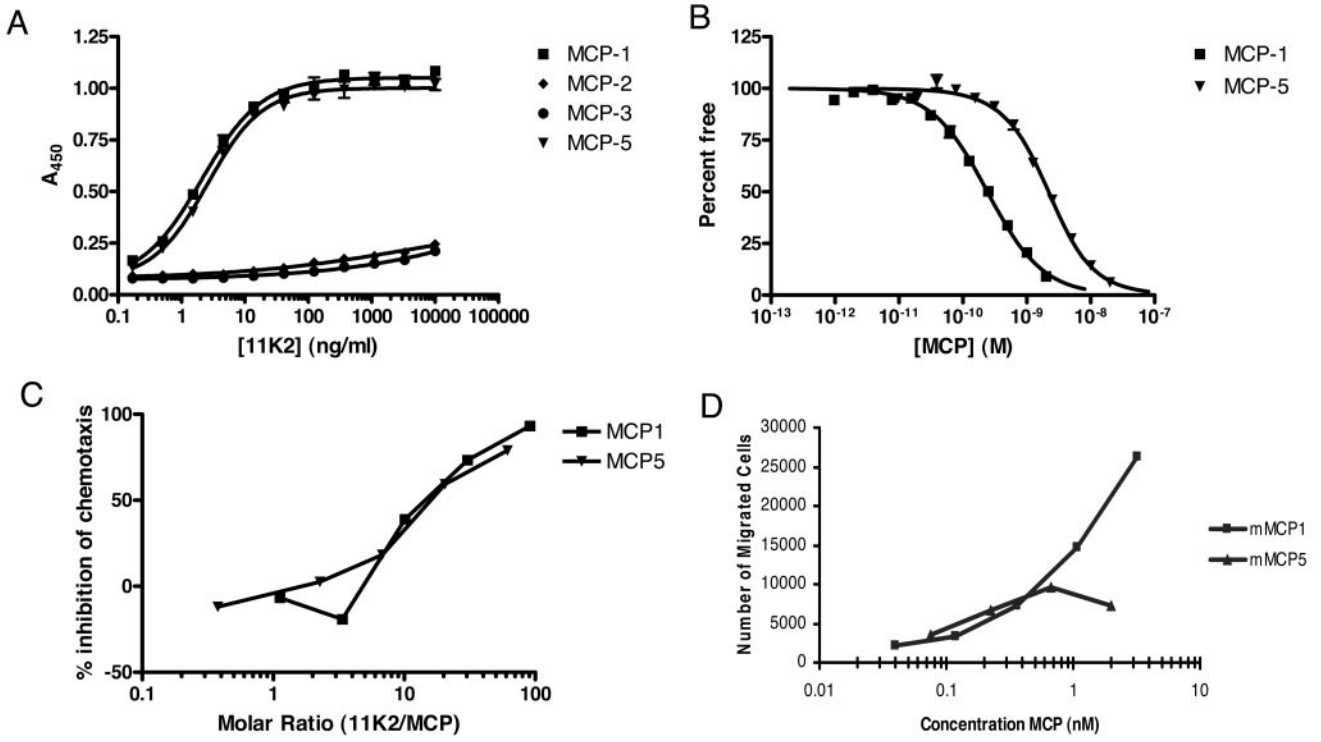

Figure 3. 11K2 is a binding antagonist of murine MCP-1 and MCP-5. A, Binding of 11K2 to surface-coated murine MCP-1, MCP-2, MCP-3, and MCP-5 measured by ELISA. B, Measurement of free 11K2 Fab in mixtures of 11K2 Fab and MCP-1 or MCP-5 at various concentrations. C, 11K2 blocks the chemotaxis of a murine monocytic cell line induced by murine MCP-1 and MCP-5. D, Both MCP-1 and MCP-5 are strong chemotactic agents for monocytes.

tested for the inhibition of murine monocyte migration across a filter barrier over a 4-hour test period. For both murine MCP-1 and MCP-5, a 50% reduction in migration was observed with ≈20-fold excess of monoclonal antibody (Figure 3C).

Role of MCP-1 and MCP-5 in Monocyte Recruitment

In an in vitro experiment using THP-1 cells, we showed that both MCP-1 and MCP-5 are strong mediators of monocyte recruitment (Figure 3D). These results indicate an important role for both MCP-1 and MCP-5 in monocyte recruitment in atherosclerotic plaques.

Mouse Study

In the early treatment group (treatment from age 5 to 17 weeks), survival rates were 100%. In the delayed treatment group (treatment from age 17 to 29 weeks), survival rates were 93.3% for the 11k2-treated group and 93.3% for the control-treated group. Macroscopic and microscopic analysis on hematoxylin-eosin–stained sections of >20 organs revealed no abnormalities. No differences in total cholesterol, triglycerides, HDL, and LDL were observed between 11K2- and control-treated ApoE$^{-/-}$ mice (data not shown).

FACS analysis on peripheral blood leukocytes, spleen, and lymph nodes revealed no differences in the number of CD3$^+$ cells or in the activation status of T cells (CD4$^+$/CD8$^+$ ratio, CD25$^+$ T cells) between 11K2- and control-treated ApoE$^{-/-}$ mice (data not shown).

Plaque Development and Phenotype

In the early treatment group (treatment age 5 to 17 weeks), 11K2 treatment decreased total atherosclerotic plaque area per aortic arch (Figure 4A).

After this treatment regimen, only initial lesions were present in the aortic arch of 11K2- and control-treated ApoE$^{-/-}$ mice. Although the number of initial lesions per aortic arch did not change after 11K2 treatment (2.1±0.2 lesions per aortic arch for 11K2 versus 2.2±0.4 for control), these initial lesions were remarkably smaller in 11K2-treated mice than in control-treated mice (8.803±1.314 μm^2 for 11K2 versus 12.921±1.258 μm^2 for control; $P<0.05$). This indicates that 11K2 treatment does not impair lesion initiation but does inhibit lesion growth.

In the delayed treatment group (treatment from age 17 to 29 weeks), we also observed a significant decrease in total plaque area per aortic arch after 11K2 treatment (Figure 4A). Although individual initial and advanced plaque area did not change after 11K2 treatment, the total number of advanced plaques per aortic arch significantly decreased (2.6±0.3 for 11K2 versus 4.0±0.2 for control; $P<0.05$), whereas the number of initial lesions increased (1.9±0.3 for 11K2 versus 1.1±0.2 for control). This indicates that the decrease in total plaque area is due to inhibition of disease progression: initial lesions partly fail to progress into advanced atherosclerotic plaques.

A third observation that stresses the effect of 11K2 treatment on lesion progression is that the increase in plaque

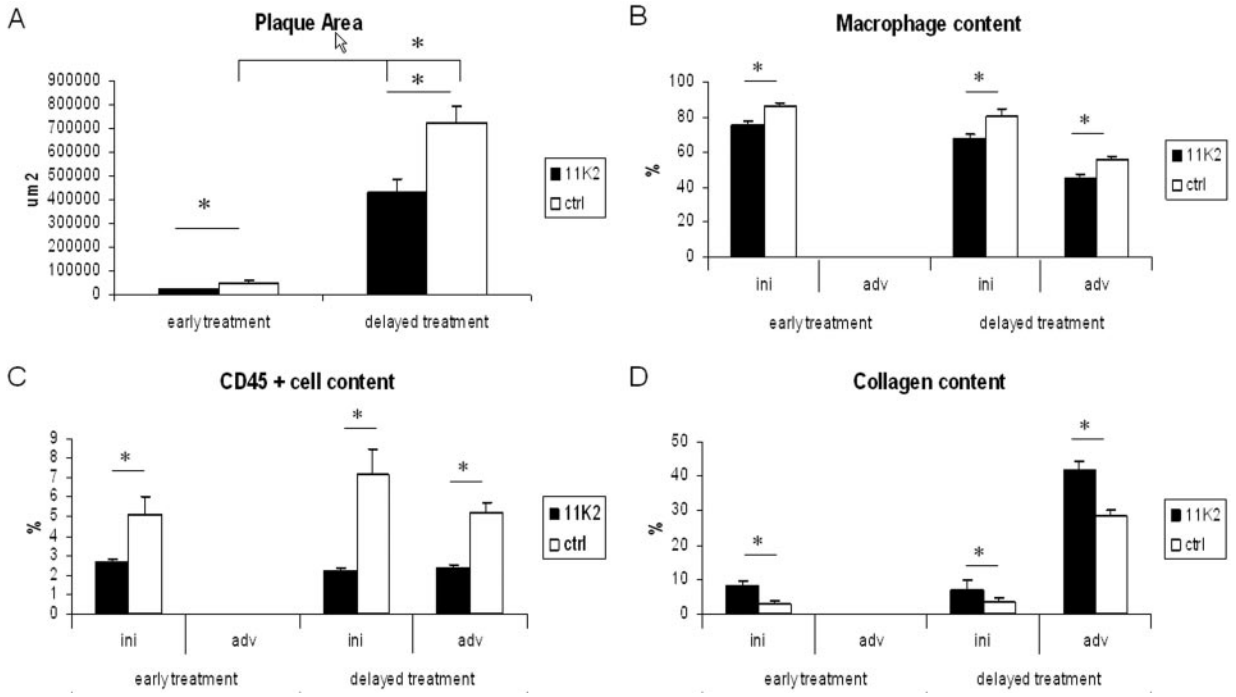

Figure 4. Plaque characteristics of ApoE$^{-/-}$ mice treated with 11K2 or a control (ctrl) antibody. A, 11K2 treatment significantly decreased total plaque area per aortic arch. B, C, Macrophage content and CD45^{+} cell content significantly decreased in initial (ini) and advanced (adv) lesions after 11K2 treatment. D, Collagen content significantly increased in initial and advanced lesions after 11K2 treatment. *$P<0.05$.

area was retarded from 14.1-fold from week 17 to week 29 in the control group to only 8.3-fold in the 11K2-treated group (Figure 4A).

Analysis of plaque composition showed that early and advanced atherosclerotic plaques of ApoE$^{-/-}$ mice treated with the 11K2 antibody were particularly low in inflammation. Both initial and advanced atherosclerotic lesions of early and delayed treatment groups showed a profound reduction in macrophage and CD45^{+} cell content (Figure 4B, 4C, 5A to 5D). Moreover, plaques exhibited increased fibrosis after 11K2 treatment, as shown by their collagen content (Figure 4D, 5D to 5E). α-Smooth muscle actin content had increased in initial plaques after 11K2 treatment (early treatment, $4.4\pm1.2\%$ for 11K2 versus $0.7\pm0.3\%$ for control; delayed treatment, $3.3\pm1.0\%$ for 11K2 versus $0.2\pm0.1\%$ for control).

These data show that 11K2 treatment not only inhibits atherosclerotic plaque progression but also induces a plaque phenotype that is low in inflammation and high in fibrosis, which are characteristics of a stable atherosclerotic plaque.

Discussion

In the present study we obtained a detailed gene expression profile of murine atherosclerosis. We showed that each stage of atherosclerosis is characterized by a unique but complex expression pattern of genes. Time-related expression clustering and functional grouping of genes shed some light on these complex patterns.

The uniqueness of gene expression profiles during atherosclerosis is reflected by the outcome of a similar experiment performed with wild-type mice. In that study we analyzed gene profiles of aortic arches of C57Bl6 mice of ages and diets similar to those of the present study. Remarkably, only 107 genes were differentially expressed, most of them selectively in C57Bl6, and only a few unannotated clusters could be identified (data not shown).

The 2 largest clusters/functional gene groups identified during atherogenesis were those of inflammation and proteolysis. Within these 2 groups, 2 gene families in particular were modulated during atherogenesis: the small inducible cytokines and the cathepsins. Broad-range inhibitors of both families may therefore be considered valuable targets for the treatment of atherosclerosis, especially because inhibition of individual genes showed promising results.

Small inducible cytokines or chemokines are members of a superfamily of small secreted proteins (8 to 16 kDa) that mediate migration and activation of inflammatory cells into the tissue.[24] Members of the CC chemokine subfamily (MCP-1, MCP-2, MCP-5, MIP-1α, MIP-1β, MIP-3α, MIP-3β, RANTES, eotaxin, TECK, CCL21a+b) predominantly chemoattract monocytes and T lymphocytes but not neutrophils. Members of the CXC family (IL-8, SDF-1, MIP-2, CXCL16) particularly induce the migration of neutrophils and not monocytes. Fractalkine, the only CX3C chemokine described, not only functions as a chemoattractant but also acts as an adhesion molecule. The XCL chemokine lymphotactin induces T-cell trafficking.[24]

Most of the chemokines reported are present in human atherosclerotic plaques.[25] Moreover, a subset of the chemokine family has been tested in atherosclerotic animal models and proved an important role for this family in the pathogenesis of atherosclerosis. Atherosclerotic mice that functionally lack MCP-1,[26,27] RANTES,[28] or the chemokine receptors

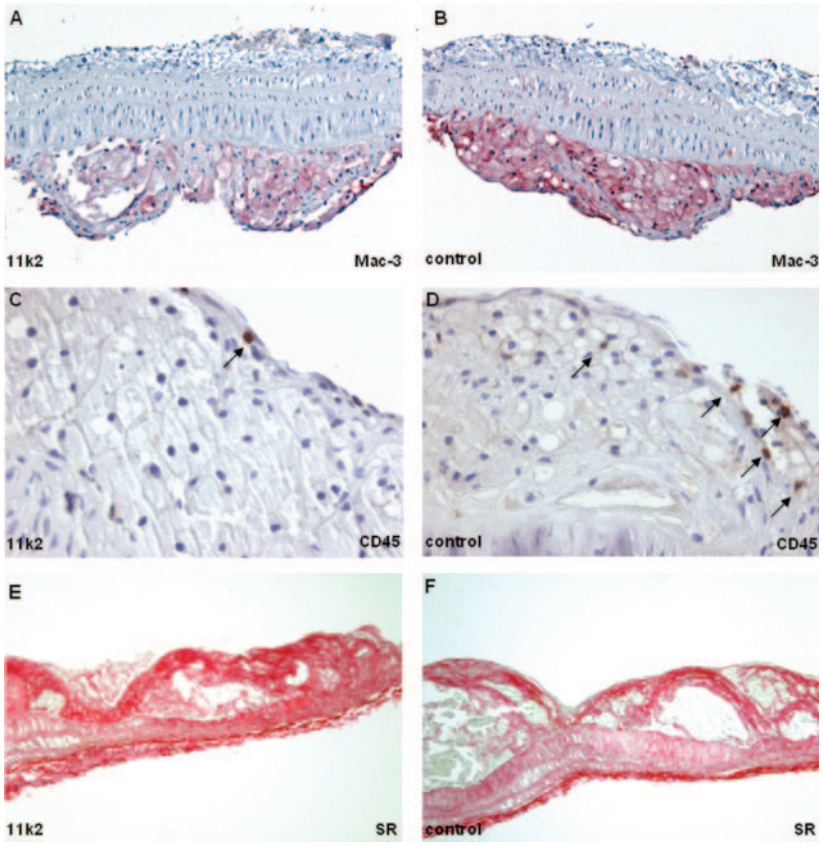

Figure 5. Mac-3 staining (magnification ×200) of intermediate atherosclerotic plaques is shown. The relative amount of Mac-3$^+$ macrophages is decreased after 11K2 treatment (A) compared with control treatment (B). CD45 staining (magnification ×400) of advanced atherosclerotic lesions (shoulder region) is shown. 11K2 treatment (C) resulted in a decrease in percentage of CD45$^+$ leukocytes (arrows) compared with control treatment (D). Sirius red (SR) staining (magnification ×100) of advanced atherosclerotic plaques reveals an increase in collagen content after 11K2 treatment (E) compared with control treatment (F).

CCR-2,[29,30] CXCR2,[31] and CX3CR1[32,33] reduced atherosclerosis. Moreover, inhibition of most of these chemokines reduced the inflammatory cell content in the lesion and induced an increase in extracellular matrix content, characteristics of a stable atherosclerotic plaque. An exception is the chemokine receptor CCR-5, which failed to affect atherosclerosis.[34] The recently discovered IFN-γ–regulated chemokine CXCL16 was also found to be expressed in atherosclerosis.[35]

In the present study we found that even more members of the small inducible cytokine family were present in atherosclerotic lesions. Besides upregulation of MCP-1 and fractalkine, we also found upregulation of MCP-3, MCP-5, MIP-1α, MIP-1β, and IL-8-like. Interestingly, in contrast to an earlier report,[28] we found downregulation of RANTES and of CCL21a and CCL21b, especially in the more advanced stages of atherosclerosis. Our microarray results stress the importance of the entire gene family of small inducible cytokines in atherosclerosis.

In a subsequent in vivo experiment, we designed a unique inhibitor (11K2) for the small inducible cytokines MCP-1 and MCP-5. MCP-1 and MCP-5 both bind to the CCR-2 receptor.[36] Administration of 11K2 to ApoE$^{-/-}$ mice in a prevention and a regression setting revealed that inhibition of MCP-1 and MCP-5 resulted in reduction of atherosclerosis. Moreover, atherosclerotic plaques were low in inflammation and contained increased amounts of extracellular matrix. Inhibition of MCP-1 and MCP-5 induced a stable atherosclerotic plaque phenotype.

Although our antibody did not distinguish between the individual effects of MCP-1 and MCP-5, we showed that both MCP-1 and MCP-5 are potent monocyte chemoattractants in vitro, suggesting an important role for both MCP-1 and MCP-5 in monocyte recruitment in atherosclerotic plaques in vivo. Unfortunately, we could not perform comparative experiments in vivo because we would need a humanized anti-murine MCP-1 and/or MCP-5 monoclonal antibody for comparison with 11k2, neither of which exist at present. The only available monoclonal antibody specifically against MCP-1 is a hamster anti-rodent antibody (clone 2H5).[37] Hamster monoclonal antibodies are notoriously antigenic in mice and are therefore not suitable for long-term in vivo experiments.

Although our mouse data are very promising, caution should be exercised in regard to the use of 11K2 as treatment of human atherosclerosis. Atherosclerosis is a slowly progressive disease, and therefore long-term treatment is required. One of the problems with long-term application of antibodies is the development of "anti-drug" antibodies. Moreover, antibodies are large proteins, and the risk of nonspecific binding to other epitopes is present. MCP-1 and MCP-5 are also involved in combating infections; therefore, safety of long-term 11K2 treatment might be questionable. However, FACS analysis in our mice did not reveal any signs of immunosuppression after a 3-month treatment period. Recently, antibody therapy in small groups of patients with the use of antibodies against tumor necrosis factor-α, CD40L, and interleukin-12 for Crohn's disease, rheumatoid arthritis, and systemic lupus erythematosus proved effective with only limited side effects.[38–40]

For the cluster subfamily of cathepsins, which are important cysteine proteases, we observed that cathepsin B, D, H,

L, S, and Z were highly expressed during atherogenesis. Cathepsin S was one of the most highly expressed genes of our microarray in all stages of atherosclerosis. Cathepsin B, D, L, S, and K were previously reported to be expressed in atherosclerotic plaques.[41,42] Mice deficient in cathepsin S and the LDL receptor showed a decrease in plaque area, plaque macrophage, smooth muscle cell, and T-lymphocyte content,[43] indicating an important role of cathepsin S in atherosclerotic plaque progression.

Besides the 2 most abundant functional clusters, functional gene groups like blood coagulation (eg, Gas6), cholesterol metabolism (eg, fatty acid binding protein), embryogenesis, and morphogenesis (homeobox genes, dickkopf homolog 3) were also significantly activated, reflecting the highly complex nature of atherosclerotic plaque development and progression.

Microarrays are becoming increasingly integral in unraveling pathways of complex diseases. Although they are powerful, caution must exercised in regard to the experimental design and interpretation of results. Before multiple microarray measurements can be integrated into a single analysis, measurements of individual arrays must be normalized.[44] In our study we used a pool of cDNA derived from ApoE$^{-/-}$ mice fed NC for 3 months that was used as a reference for all microarrays. In each microarray experiment, there is a significant amount of "biological noise" that can distort the interpretation of the expression data.[44] To avoid misinterpretation, microarrays were performed in duplicate, and the expression of a subset of genes was validated with real-time PCR, ELISA, and immunohistochemistry.

Despite our careful analysis and validation experiments, the use of entire aortic arches in the analysis implies that both intima and media may contribute to the observed differences in gene expression. However, validation experiments for our candidate genes did not show expression in the media.

Moreover, in our present setup, differential gene expression of individual cell types in the plaque (smooth muscle cells, macrophages, endothelial cells, T lymphocytes) could only be distinguished after validation. A method successfully used to identify gene expression profiles of individual plaque cell types, macrophages in this case, is microdissection of individual cells by laser capture microscopy.[10,45]

In the present study we show that the use of DNA microarray analysis yielded a detailed database that will improve insight into the pathogenesis of atherosclerosis and will be helpful to identify new diagnostic markers and therapeutic targets to monitor and intervene in atherosclerotic plaque progression.

Acknowledgments

Dr Lutgens is a postdoctoral fellow of the Dr E. Dekker program of the Dutch Heart Foundation (2000T41). We thank Teresa Cachero, Fang Qian, Joseph Amatucci, and Konrad Miatkowski (Biogen Idec) for reagent purification and characterization.

References

1. Zhang QJ, Goddard M, Shanahan C, Shapiro L, Bennett M. Differential gene expression in vascular smooth muscle cells in primary atherosclerosis and in stent stenosis in humans. *Arterioscler Thromb Vasc Biol*. 2002;22:2030–2036.
2. Feng Y, Yang JH, Huang H, Kennedy SP, Turi TG, Thompson JF, Libby P, Lee RT. Transcriptional profile of mechanically induced genes in human vascular smooth muscle cells. *Circ Res*. 1999;85:1118–1123.
3. de Vries CJ, van Achterberg TA, Horrevoets AJ, ten Cate JW, Pannekoek H. Differential display identification of 40 genes with altered expression in activated human smooth muscle cells: local expression in atherosclerotic lesions of smags, smooth muscle activation–specific genes. *J Biol Chem*. 2000;275:23939–23947.
4. Shiffman D, Mikita T, Tai JT, Wade DP, Porter JG, Seilhamer JJ, Somogyi R, Liang S, Lawn RM. Large scale gene expression analysis of cholesterol-loaded macrophages. *J Biol Chem*. 2000;275:37324–37332.
5. Herman MP, Sukhova GK, Libby P, Gerdes N, Tang N, Horton DB, Kilbride M, Breitbart RE, Chun M, Schonbeck U. Expression of neutrophil collagenase (matrix metalloproteinase-8) in human atheroma: a novel collagenolytic pathway suggested by transcriptional profiling. *Circulation*. 2001;104:1899–1904.
6. Adams LD, Geary RL, McManus B, Schwartz SM. A comparison of aorta and vena cava medial message expression by cDNA array analysis identifies a set of 68 consistently differentially expressed genes, all in aortic media. *Circ Res*. 2000;87:623–631.
7. Geary RL, Wong JM, Rossini A, Schwartz SM, Adams LD. Expression profiling identifies 147 genes contributing to a unique primate neointimal smooth muscle cell phenotype. *Arterioscler Thromb Vasc Biol*. 2002;22:2010–2016.
8. Martinet W, Schrijvers DM, De Meyer GR, Thielemans J, Knaapen MW, Herman AG, Kockx MM. Gene expression profiling of apoptosis-related genes in human atherosclerosis: upregulation of death-associated protein kinase. *Arterioscler Thromb Vasc Biol*. 2002;22:2023–2029.
9. Tyson KL, Weissberg PL, Shanahan CM. Heterogeneity of gene expression in human atheroma unmasked using cDNA representational difference analysis. *Physiol Genomics*. 2002;9:121–130.
10. Tuomisto TT, Korkeela A, Rutanen J, Viita H, Brasen JH, Riekkinen MS, Rissanen TT, Karkola K, Kiraly Z, Kolble K, Yla-Herttuala S. Gene expression in macrophage-rich inflammatory cell infiltrates in human atherosclerotic lesions as studied by laser microdissection and DNA array: overexpression of HMG-CoA reductase, colony stimulating factor receptors, CD11A/CD18 integrins, and interleukin receptors. *Arterioscler Thromb Vasc Biol*. 2003;23:2235–2240.
11. Ross R. Atherosclerosis: an inflammatory disease. *N Engl J Med*. 1999;340:115–126.
12. Lusis AJ. Atherosclerosis. *Nature*. 2000;407:233–241.
13. Faber BC, Cleutjens KB, Niessen RL, Aarts PL, Boon W, Greenberg AS, Kitslaar PJ, Tordoir JH, Daemen MJ. Identification of genes potentially involved in rupture of human atherosclerotic plaques. *Circ Res*. 2001;89:547–554.
14. Bijnens AP, Gils A, Jutten B, Faber BC, Heeneman S, Kitslaar PJ, Tordoir JH, de Vries CJ, Kroon AA, Daemen MJ, Cleutjens KB. Vasculin, a novel vascular protein differentially expressed in human atherogenesis. *Blood*. 2003;102:2803–2810.
15. Randi AM, Biguzzi E, Falciani F, Merlini P, Blakemore S, Bramucci E, Lucreziotti S, Lennon M, Faioni EM, Ardissino D, Mannucci PM. Identification of differentially expressed genes in coronary atherosclerotic plaques from patients with stable or unstable angina by cDNA array analysis. *J Thromb Haemost*. 2003;1:829–835.
16. Wuttge DM, Sirsjo A, Eriksson P, Stemme S. Gene expression in atherosclerotic lesion of ApoE deficient mice. *Mol Med*. 2001;7:383–392.
17. Tabibiazar R, Wagner RA, Spin JM, Ashley EA, Narasimhan B, Rubin EM, Efron B, Tsao PS, Tibshirani R, Quertermous T. Mouse strain–specific differences in vascular wall gene expression and their relationship to vascular disease. *Arterioscler Thromb Vasc Biol*. 2005;25:302–308.
18. Lutgens E, Gorelik L, Daemen MJ, de Muinck ED, Grewal IS, Koteliansky VE, Flavell RA. Requirement for CD154 in the progression of atherosclerosis. *Nat Med*. 1999;5:1313–1316.
19. Pabon C, Modrusan Z, Ruvolo MV, Coleman IM, Daniel S, Yue H, Arnold LJ Jr. Optimized T7 amplification system for microarray analysis. *Biotechniques*. 2001;31:874–879.
20. DeRisi JL, Iyer VR, Brown PO. Exploring the metabolic and genetic control of gene expression on a genomic scale. *Science*. 1997;278:680–686.
21. Dahlquist KD, Salomonis N, Vranizan K, Lawlor SC, Conklin BR. GenMAPP, a new tool for viewing and analyzing microarray data on biological pathways. *Nat Genet*. 2002;31:19–20.
21a. Hulme EC, Birdsall NJM. Strategy and tactics in receptor-binding studies. In: Holme EC, ed. *Receptor Ligand Interactions: A Practical Approach.*. New York, NY: Oxford University Press; 1992:63–176.

22. Lutgens E, Gijbels M, Smook M, Heeringa P, Gotwals P, Koteliansky VE, Daemen MJ. Transforming growth factor-beta mediates balance between inflammation and fibrosis during plaque progression. *Arterioscler Thromb Vasc Biol*. 2002;22:975–982.
23. Virmani R, Kolodgie FD, Burke AP, Farb A, Schwartz SM. Lessons from sudden coronary death: a comprehensive morphological classification scheme for atherosclerotic lesions. *Arterioscler Thromb Vasc Biol*. 2000; 20:1262–1275.
24. Rossi D, Zlotnik A. The biology of chemokines and their receptors. *Annu Rev Immunol*. 2000;18:217–242.
25. Sheikine Y, Hansson GK. Chemokines and atherosclerosis. *Ann Med*. 2004;36:98–118.
26. Ni W, Egashira K, Kitamoto S, Kataoka C, Koyanagi M, Inoue S, Imaizumi K, Akiyama C, Nishida KI, Takeshita A. New anti-monocyte chemoattractant protein-1 gene therapy attenuates atherosclerosis in apolipoprotein E–knockout mice. *Circulation*. 2001;103:2096–2101.
27. Inoue S, Egashira K, Ni W, Kitamoto S, Usui M, Otani K, Ishibashi M, Hiasa K, Nishida K, Takeshita A. Anti-monocyte chemoattractant protein-1 gene therapy limits progression and destabilization of established atherosclerosis in apolipoprotein E–knockout mice. *Circulation*. 2002;106:2700–2706.
28. Veillard NR, Kwak B, Pelli G, Mulhaupt F, James RW, Proudfoot AE, Mach F. Antagonism of RANTES receptors reduces atherosclerotic plaque formation in mice. *Circ Res*. 2004;94:253–261.
29. Boring L, Gosling J, Cleary M, Charo IF. Decreased lesion formation in CCR2−/− mice reveals a role for chemokines in the initiation of atherosclerosis. *Nature*. 1998;394:894–897.
30. Guo J, Van Eck M, Twisk J, Maeda N, Benson GM, Groot PH, Van Berkel TJ. Transplantation of monocyte CC-chemokine receptor 2–deficient bone marrow into ApoE3-Leiden mice inhibits atherogenesis. *Arterioscler Thromb Vasc Biol*. 2003;23:447–453.
31. Boisvert WA, Santiago R, Curtiss LK, Terkeltaub RA. A leukocyte homologue of the IL-8 receptor CXCR-2 mediates the accumulation of macrophages in atherosclerotic lesions of LDL receptor–deficient mice. *J Clin Invest*. 1998;101:353–363.
32. Combadiere C, Potteaux S, Gao JL, Esposito B, Casanova S, Lee EJ, Debre P, Tedgui A, Murphy PM, Mallat Z. Decreased atherosclerotic lesion formation in CX3CR1/apolipoprotein E double knockout mice. *Circulation*. 2003;107:1009–1016.
33. Lesnik P, Haskell CA, Charo IF. Decreased atherosclerosis in CX3CR1−/− mice reveals a role for fractalkine in atherogenesis. *J Clin Invest*. 2003;111:333–340.
34. Kuziel WA, Dawson TC, Quinones M, Garavito E, Chenaux G, Ahuja SS, Reddick RL, Maeda N. CCR5 deficiency is not protective in the early stages of atherogenesis in apoE knockout mice. *Atherosclerosis*. 2003; 167:25–32.
35. Wuttge DM, Zhou X, Sheikine Y, Wagsater D, Stemme V, Hedin U, Stemme S, Hansson GK, Sirsjo A. CXCL16/SR-PSOX is an interferon-gamma–regulated chemokine and scavenger receptor expressed in atherosclerotic lesions. *Arterioscler Thromb Vasc Biol*. 2004;24:750–755.
36. Sarafi MN, Garcia-Zepeda EA, MacLean JA, Charo IF, Luster AD. Murine monocyte chemoattractant protein (MCP)-5: a novel CC chemokine that is a structural and functional homologue of human MCP-1. *J Exp Med*. 1997;185:99–109.
37. Luo Y, Laning J, Hayashi M, Hancock PR, Rollins B, Dorf ME. Serologic analysis of the mouse beta chemokine JE/monocyte chemoattractant protein-1. *J Immunol*. 1994;153:3708–3716.
38. Mannon PJ, Fuss IJ, Mayer L, Elson CO, Sandborn WJ, Present D, Dolin B, Goodman N, Groden C, Hornung RL, Quezado M, Neurath MF, Salfeld J, Veldman GM, Schwertschlag U, Strober W. Anti-interleukin-12 antibody for active Crohn's disease. *N Engl J Med*. 2004; 351:2069–2079.
39. St Clair EW, van der Heijde DM, Smolen JS, Maini RN, Bathon JM, Emery P, Keystone E, Schiff M, Kalden JR, Wang B, Dewoody K, Weiss R, Baker D. Combination of infliximab and methotrexate therapy for early rheumatoid arthritis: a randomized, controlled trial. *Arthritis Rheum*. 2004;50:3432–3443.
40. Grammer AC, Slota R, Fischer R, Gur H, Girschick H, Yarboro C, Illei GG, Lipsky PE. Abnormal germinal center reactions in systemic lupus erythematosus demonstrated by blockade of CD154-CD40 interactions. *J Clin Invest*. 2003;112:1506–1520.
41. Jormsjo S, Wuttge DM, Sirsjo A, Whatling C, Hamsten A, Stemme S, Eriksson P. Differential expression of cysteine and aspartic proteases during progression of atherosclerosis in apolipoprotein E–deficient mice. *Am J Pathol*. 2002;161:939–945.
42. Sukhova GK, Shi GP, Simon DI, Chapman HA, Libby P. Expression of the elastolytic cathepsins S and K in human atheroma and regulation of their production in smooth muscle cells. *J Clin Invest*. 1998;102: 576–583.
43. Sukhova GK, Zhang Y, Pan JH, Wada Y, Yamamoto T, Naito M, Kodama T, Tsimikas S, Witztum JL, Lu ML, Sakara Y, Chin MT, Libby P, Shi GP. Deficiency of cathepsin S reduces atherosclerosis in LDL receptor–deficient mice. *J Clin Invest*. 2003;111:897–906.
44. Butte A. The use and analysis of microarray data. *Nat Rev Drug Discov*. 2002;1:951–960.
45. Trogan E, Choudhury RP, Dansky HM, Rong JX, Breslow JL, Fisher EA. Laser capture microdissection analysis of gene expression in macrophages from atherosclerotic lesions of apolipoprotein E–deficient mice. *Proc Natl Acad Sci U S A*. 2002;99:2234–2239.